METRICA
METRology Institutional CAtalog

ISTITUTO NAZIONALE DI RICERCA METROLOGICA
Repository Istituzionale

Removal of sulfanilamide by tailor-made magnetic metal-ceramic nanocomposite adsorbents

This is the author's submitted version of the contribution published as:

Original
Removal of sulfanilamide by tailor-made magnetic metal-ceramic nanocomposite adsorbents / Sannino, Filomena; Pansini, Michele; Marocco, Antonello; Cinquegrana, Alessia; Esposito, Serena; Tammaro, Olimpia; Barrera, Gabriele; Tiberto, Paola; Allia, Paolo; Pirozzi, Domenico. - In: JOURNAL OF ENVIRONMENTAL MANAGEMENT. - ISSN 0301-4797. - 310:(2022), p. 114701. [10.1016/j.jenvman.2022.114701]
Availability:
This version is available at: 11696/75947 since: 2023-06-28T14:59:00Z

Publisher:
ACADEMIC PRESS LTD- ELSEVIER SCIENCE LTD

Published
DOI:10.1016/j.jenvman.2022.114701

Terms of use:

This article is made available under terms and conditions as specified in the corresponding bibliographic description in the repository

Publisher copyright

(Article begins on next page)

12 August 2023

Journal of Environmental Management

Removal of sulfanilamide by tailor-made magnetic metal-ceramic nanocomposite adsorbents

--Manuscript Draft--

Manuscript Number:	JEMA-D-21-08739
Article Type:	Research Article
Keywords:	wastewater remediation antibiotic removal magnetic metal-ceramic nanocomposites thermal regeneration
Abstract:	Three tailor-made magnetic metal-ceramic nanocomposites, obtained from zeolite A and a natural clinoptilolite, have been used as adsorbents to remove sulfanilamide (SA), a sulfonamide antibiotic of common use, from water. A patented process for the synthesis of nanocomposites has been suitably modified to maximize the efficiency of the sulfanilamide removal, as well as to extend the applicability of the materials. The role played by the main process parameters (kinetic, pH, initial concentration of SA) has been characterized. The SA removal was strongly affected by pH suggesting the adsorption mechanism to be based on an acid-base reactions. The adsorption kinetics were in all cases described by the pseudo second-order model. The adsorption isotherms data were satisfactorily described by the Langmuir and Freundlich model, suggesting that the monolayer adsorption of sulfanilamide on the magnetic nanocomposites results from an uniform surface energy. On the basis of the TG and DTA characterization of SA, an effective procedure for the thermal regeneration of the exhausted adsorbent was developed, ensuring an effective removal of the antibiotic and a proper recycle of the magnetic adsorbents.

Powered by Editorial Manager® and ProduXion Manager® from Aries Systems Corporation

REMOVAL OF SULFANILAMIDE BY TAILOR-MADE MAGNETIC METAL-CERAMIC NANOCOMPOSITE ADSORBENTS

Filomena Sannino[1], Michele Pansini[2], Antonello Marocco[2], Alessia Cinquegrana[3], Serena Esposito[4], Gabriele Barrera[5], Paola Tiberto[5], Paolo Allia[4, 5], Domenico Pirozzi[3]

[1]*University of Naples "Federico II", Department of Agricultural Sciences, Via Università 100, 80055 Portici (Naples, Italy)*
[2]*Department of Civil and Mechanical Engineering and INSTM Research Unit, Università degli Studi di Cassino e del Lazio Meridionale, Via G. Di Biasio 43, 03043 Cassino, FR, Italy*
[3]*University of Naples "Federico II", Department of Chemical Engineering, Materials and Industrial Production (DICMaPI), Laboratory of Biochemical Engineering. Piazzale Tecchio, 80, 80125, Naples (Italy)*
[4] *Department of Applied Science and Technology and INSTM Unit of Torino – Politecnico, Politecnico di Torino, Corso Duca degli Abruzzi 24, 10129, Torino, Italy.*
[5]*INRiM Torino, Advanced Materials for Metrology and Life Sciences, Strada delle Cacce 91, 10143 Torino, Italy*

Corresponding author:

Prof. Domenico Pirozzi dpirozzi@unina.it
Department of Chemical, Materials and Production Engineering (DICMAPI)
Università di Napoli "Federico II
Piazzale Tecchio 80, 80125 Napoli, Italy
Phone: +390817682274.

Graphical Abstracts

Click here to download Graphical Abstracts graphical abstract.pdf

- Cation exchange
- Thermal treatment under reducing atmosphere

Zeolite

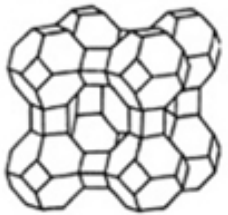

Tailor-made magnetic nanocomposite

adsorbed sulfanilamide

adsorption

desorption

sulfanilamide

- Thermal treatment

Highlights

- Three tailor-made magnetic metal-ceramic nanocomposites were obtained from zeolites
- The adsorption by magnetic adsorbents was affected by acid-base reactions
- A thermal regeneration treatment of the adsorbent was developed
- The magnetic adsorbents could be easily separated and regenerated

Manuscript
Click here to download Manuscript 2021_10_13 manuscript Sannino et al.doc

REMOVAL OF SULFANILAMIDE BY TAILOR-MADE MAGNETIC METAL-CERAMIC NANOCOMPOSITE ADSORBENTS

Filomena Sannino[1], Michele Pansini[2], Antonello Marocco[2], Alessia Cinquegrana[3], Serena Esposito[4], Gabriele Barrera[5], Paola Tiberto[5], Paolo Allia[4, 5], Domenico Pirozzi[3]

[1]University of Naples "Federico II", Department of Agricultural Sciences, Via Università 100, 80055 Portici (Naples, Italy)
[2]Department of Civil and Mechanical Engineering and INSTM Research Unit, Università degli Studi di Cassino e del Lazio Meridionale, Via G. Di Biasio 43, 03043 Cassino, FR, Italy
[3]University of Naples "Federico II", Department of Chemical Engineering, Materials and Industrial Production (DICMaPI), Laboratory of Biochemical Engineering. Piazzale Tecchio, 80, 80125, Naples (Italy)
[4] Department of Applied Science and Technology and INSTM Unit of Torino – Politecnico, Politecnico di Torino, Corso Duca degli Abruzzi 24, 10129, Torino, Italy.
[5]INRiM Torino, Advanced Materials for Metrology and Life Sciences, Strada delle Cacce 91, 10143 Torino, Italy

Corresponding author:

Prof. Domenico Pirozzi dpirozzi@unina.it
Department of Chemical, Materials and Production Engineering (DICMAPI)
Università di Napoli "Federico II
Piazzale Tecchio 80, 80125 Napoli, Italy
Phone: +390817682274.

Abstract

Three tailor-made magnetic metal-ceramic nanocomposites, obtained from zeolite A and a natural clinoptilolite, have been used as adsorbents to remove sulfanilamide (SA), a sulfonamide antibiotic of common use, from water.

A patented process for the synthesis of nanocomposites has been suitably modified to maximize the efficiency of the sulfanilamide removal, as well as to extend the applicability of the materials.

The role played by the main process parameters (kinetic, pH, initial concentration of SA) has been characterized. The SA removal was strongly affected by pH suggesting the adsorption mechanism to be based on an acid-base reactions.

The adsorption kinetics were in all cases described by the pseudo second-order model. The adsorption isotherms data were satisfactorily described by the Langmuir and Freundlich model, suggesting that the monolayer adsorption of sulfanilamide on the magnetic nanocomposites results from an uniform surface energy.

On the basis of the TG and DTA characterization of SA, an effective procedure for the thermal regeneration of the exhausted adsorbent was developed, ensuring an effective removal of the antibiotic and a proper recycle of the magnetic adsorbents.

Key words:magnetic metal ceramic nanocomposites, antibiotic removal, thermal regeneration

1. Introduction

Sulfonamides (sulfa drugs, SAs) are synthetic antibiotics able to inhibit both gram-positive and gram-negative bacteria. They are systematically used to treat/prevent bacterial infections (van Mil, 2011). In particular, sulfonamides antibiotics (SAs) are commonly used in human therapy, livestock production and aquaculture due to their low cost and good effect (Dibner and Richards, 2005; Neu and Gootz, 1996).

Unfortunately, the spread of sulfonamides has led to the increase of human allergies and drug-resistance bacteria. They can also deteriorate the quality of drinking water and may cause potential hazard (carcinogenicity, teratogenicity and mutagenicity) (Qin et al., 2020). Recently, antibiotics have been detected in natural waters at concentration levels going from ng/L to µg/L (Sabri et al., 2020; Zhou et al., 2019; Conde-Cid et al., 2021; Dekhi-Bemani et al., 2021). For this reason they have been declared as priority substances in water protection policies (Directive 2013/39/EU),

Several technologies have been developed to remove these contaminants such as coagulation, sedimentation, advanced oxidation processes, filtration, membrane technologies, and biological treatments (Ortiz et al., 2015; Kassinos et al., 2011; Pirozzi et al., 2020; Sannino et al., 2014; Sannino et al., 2015). However, most of these processes imply the transfer of the pollutants between different fluid phases, use of additional chemicals or high amounts of energy during the process and generate wastes and byproducts that have to be disposed in subsequent steps. Adsorption is considered an excellent method for treating wastewater containing low concentration of antibiotics on account of its high efficiency, intrinsic simplicity, antitoxic nature and low cost (Srivastava et al., 2009; De Gisi et al., 2016; Sannino et al., 2013a; Addorisio et al., 2011).

A point of weakness of the adsorption procedures, still limiting their full application, stems from the difficult separation of the exhausted adsorbent from water. This consideration suggested us to develop magnetic metal-ceramic nano-composites as adsorbents, that could be easily separated from the aqueous phase by the action of an external magnetic field.

In this view, tailor-made nano-composites have been produced starting from a zeolite precursor, to exploit the peculiar properties of zeolites, such as high cation exchange capacity, swelling, and wide availability. Zeolites have been already used to remove SAs from wastewater (Blasioli et al., 2014).

In order to obtain these magnetic nano-composite adsorbents, a patented process (Esposito et al., 2014, 2015; Marocco et al., 2012; Ronchetti et al., 2010; Esposito et al., 2018) has been suitably modified. According to it, commercial zeolites (precursors) have been exchanged with Fe^{2+} ions.

Subsequently, the heavy-metal cation-exchanged zeolites have been thermally treated at relatively moderate temperatures (500-850 °C), under a reducing atmosphere.

During such thermal treatments, a nanocomposite formed by a dispersion of metallic Fe nanoparticles in a mainly amorphous silica and alumina matrix was obtained, showing physico-chemical properties markedly different from those of the parent zeolite. Yet, the nanocomposite exhibited a residual porosity (Esposito et al., 2018), which is a remnant of the parent zeolite structure, that may have an impact on its applications as adsorbent. The magnetic properties of the nanocomposite were confirmed in a number of studies (Barrera et al., 2018, 2019, 2020).

The process has the characteristics of a scalable method, as it implies an ionic exchange and a thermal treatment under gas flow. These nanocomposites have so far been tested in the separation of DNA from crude cell lysate (Pansini et al., 2017) and from human blood (Esposito et al., 2020), the removal of agrochemicals from water (Pansini et al., 2018; Marocco et al., 2020) and as moon dust simulant (Freyria et al., 2019; Manzoli et al., 2021), showing a large potential for further applications.

In order to maximize the efficiency of the sulfanilamide removal from water, the zeolite A and a natural clinoptilolite contained in a widespread rock (Sardinian Epiclastite) from Northern Sardinia have been selected as starting materials. In particular, the choice of A zeolites has been dictated by their high cation exchange capacity, due to their Si/Al ratio = 1.00. These zeolites have been chosen also on the basis of their large availability with consequent low cost and on the basis of the knowledge of their features.

Zeolite A and clinoptilolite have already been used used in several industrial applications (Colella et al., 1998; Pansini and Colella, 1990; Albino et al., 1995; Colella and Pansini, 1988; Cioffi et al., 1996, Pansini et al., 2010; de' Gennaro et al., 2008, Basile et al., 1992).

Three different magnetic metal-ceramic nanocomposites have been produced. The aim of this study is: i) to evaluate the ability of the magnetic nanocomposites in the removal of Sulfanilamide antibiotic (SA) from waters by adsorption, investigating the role played by the main process parameters (solid/liquid ratio, pH, time, initial concentration of SA); ii) to set up a proper regeneration procedure of the exhausted adsorbent, ensuring a depletion of the antibiotic.

2. Materials and methods

2.1. Materials

Reagent grade p-aminobenzenesulfonamide (Sulfanilamide, Scheme 1) (>99.0% purity) was from Sigma-Aldrich Chemical Company. The solvents for analytical determinations were Carlo Erba HPLC grade. Ultrapure water was used for all the experiments performed. Zeolite A (framework code LTA (Sannino et al., 2012), $Na_{12}Al_{12}Si_{12}O_{48}{\cdot}27H_2O$) in its original Na form was from Sigma-Aldrich Chemical Company.

2.2. Preparation and characterization of materials

Magnetic adsorbents were prepared starting from the following raw materials:

1) Zeolite A (framework code LTA (Sannino et al., 2012), $Na_{12}Al_{12}Si_{12}O_{48}{\cdot}27H_2O$) in its original Na form was from Sigma-Aldrich Chemical Company (the grain size distribution is reported in Cappelletti et al., 2011).
2) A clinoptilolite bearing rock from Northern Sardinia (Italy) fully characterised in a previous work (Manzoli et al., 2021).

Three different samples of magnetic metal-ceramic nanocomposites were prepared and labeled, for the sake of uniformity with previous works, as follows: (Fe,H)A800C-0min, (Fe,H)A600C-90min, and SMA_LacBen. These samples were produced by subjecting to Fe^{2+} exchange procedures the relevant zeolites and by subjecting the Fe-exchanged zeolites to the proper thermal treatment under a reducing atmosphere, according to refs. (Freyria et al., 2019; Breck, 1974). The chemical composition, quantitative phase determination, and the various characterization (SEM, TEM, textural, magnetic) are reported in refs. (Pansini et al., 2018; Freyria et al., 2019). In Table 1 the principal chemical-physical properties of the (Fe,H)A800C-0min, (Fe,H)A600C-90min, and SMA_LacBen are reported.

Scanning electron microscopy (SEM) observations of samples (Fe,H)A800C-0min, (Fe,H)A600C-90min, and SMA_LacBen were carried out on a FE-SEM Ultra Plus (Zeiss, GmbH) microscope at 20 kV (Pansini et al., 2018).

SA was subjected to simultaneous differential thermal analysis (DTA) and thermogravimetric analysis (TG) under inert atmosphere (N_2), using a Perkin-Elmer thermo-analyzer STA 6000, with Al_2O_3 as reference material. The TG and DTA tests were performed keeping 9.45 mg of SA under nitrogen atmosphere, varying the temperature from 30 to 1000 °C. A heating rate of 10 °C min^{-1} was adopted.

2.3. Analytical determination

SA concentration in solution was analyzed with an Agilent 1200 Series HPLC apparatus (Wilmington U.S.A.), equipped with a DAD array and a Chem Station Agilent Software. A Macharey-Nagel Nucleosil 100-5 C18 column (stainless steel 250 × 4 mm) was utilized. The mobile phase, a binary system of 80:20 acetonitrile: phosphate buffer (0.1% pH 2.70), was pumped at 1 mL min^{-1} flow in an isocratic mode. The detector was set at 224 nm and injection volume was 20 µL. The quantitative determination of the antibiotic was performed using a calibration curve between 1.0–1163 µmol/L.

2.4. Adsorption experiments

100 mg of SA were dissolved in 500 mL of ultrapure water. The resulting 200 mg/L (corresponding to 1163 µmol/L) solution was kept refrigerated and used to prepare all solutions tested within this work. Batch experiments of SA removal from waters by adsorption on (Fe,H)A800C–0 min, (Fe,H)A600C–90 min, and SMA_LacBen were performed. Aqueous solutions of SA were contacted with magnetic nanocomposites in glass vials with Teflon caps at 25 °C; the vessels were continuously stirred in an orbital shaker at 150 rpm until steady state conditions were approximated, which took about 24 h. Finally, the magnetic adsorbents were separated from the liquid using an external magnet (VA03, UNIDISP s.r.l. Italy) and the liquid was analysed to evaluate SA concentration, using HPLC analysis. The amount of SA adsorbed was calculated as the difference between its initial and final concentration in solution. Blanks of SA in ultrapure water were analysed in order to evaluate SA stability and sorption on vials. The following experimental factors were evaluated:

(a) Effect of pH: Magnetic nanocomposites samples, (Fe,H)A800C–0 min, (Fe,H)A600C–90 min and SMA_LacBen were contacted with 40.0 µmol/L SA solution at solid/liquid ratio (S/L) = 1/10,000 g/g for 24 h (this time was shown to be sufficient to attain a steady state). The pH of this solution varied between 2.0 and 8.0, in steps of 0.5, by adding the proper amount of 0.01 or 0.10 mmol/L HCl or NaOH aqueous solution.

(b) Adsorption kinetics: Kinetic studies were performed by contacting the SMA_LacBen adsorbent with 40.0 and 126 µmol/L SA solution, at solid/liquid ratio S/L = 1/10,000 g/g at pH 4.0 As regard the (Fe,H)A800C–0 min sample, kinetic tests were carried out with 40.0 µmol/L SA solution, at S/L = 1/10,000 g/g at pH 6.0. The suspensions were stirred for 10, 30, 60, 120, 240, 360, 900 and 1440 min and successively subjected to the separation procedure described.

(c) Sorption isotherm: Magnetic adsorbents (Fe,H)A800C–0 min and SMA_LacBen were contacted with solutions having SA concentration up to 1163 µmol/L at S/L = 1/10000 g/g, T = 25

°C and pH = 6.0 or 4.0, respectively, for 24 h. The pH of each suspension was kept constant by adding proper amounts of 0.01 or 0.10 mmol/L HCl or NaOH solution.

3. Results and Discussion

3.1. Textural and morphological characterization of (Fe,H)A800C–0min, (Fe,H)A600C–90min and SMA_LacBen

Table 1 reports the quantitative phase determinations, textural and main magnetic properties of the magnetic adsorbents (Fe,H)A800C–0min, (Fe,H)A600C–90min and SMA_LacBen. The magnetic adsorbents are formed by nanoparticles (5-30 nm) of ferromagnetic materials (Fe^0 and Fe_3O_4) dispersed in a prevailingly amorphous ceramic phase. This phase originated from the thermal collapse of the microporous zeolite structure. Such collapse is fully confirmed by the textural data. Magnetic properties of the various adsorbents were demonstrated to be sufficient to perform the separation of the solid adsorbent from the liquid (Esposito et al., 2020; Pansini et al., 2018; Freyria et al., 2019) by using a commercial external magnet. The compositional, morphologic, textural and magnetic features of the magnetic adsorbents were discussed in detail elsewhere (Pansini et al., 2018; Freyria et al., 2019) (Figure 1).

3.2. Effect of pH

The Figure 2 reports the amount of SA adsorbed on (Fe,H)A800C–0min, (Fe,H)A600C–90min and SMA_LacBen magnetic adsorbents at S/L ratio = 1/10,000 after a contact of 24 h, as a function of pH. Sulfanilamide uptake from water by the all the magnetic adsorbents tested strongly depends on pH: actually a sharp maximum is recorded at pH 6.0, 7.0 and 4.0 for (Fe,H)A800C–0min, (Fe,H)A600C–90min and SMA_LacBen, respectively, and small deviations from this value result in a marked sulfanilamide sulphonamide adsorption decrease.

This observation suggests that sulfanilamide uptake by the various adsorbents is an acid-base reaction, similar to simazine uptake from water by zeolite H-Y or porous silica (Sannino et al., 2012; Marocco et al., 2011; Sannino et al, 2013b; Esposito et al., 2013).

The effect of medium pH on the antibiotic adsorption can be explained taking into account that sulfanilamide, similarly to other sulfa drugs, undergo two acid-base processes (Boreen et al., 2004; Fukahori et al., 2013), due to the protonation and the deprotonation of the amino and sulfonamide groups as shown in the following scheme:

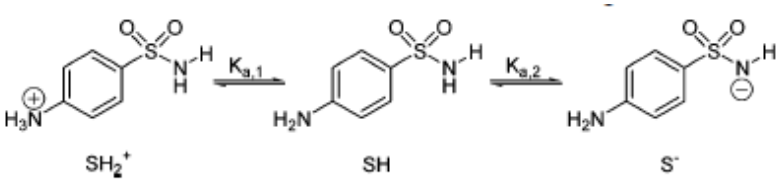

[a] SH_2^+ = cationic form, SH = neutral form, S^- = anionic form.

The protonation state is therefore described by two values of pK (Braschi et al., 2013; Uhlemann et al, 2021):

$pK_1 = 1.78$

$pK_2 = 10.6$

As a consequence, in the range of pH 4.0-7.0 most of sulfanilamide molecules are in their neutral form. This suggests that the adsorption of sulfanilamide on all the adsorbents tested is based on hydrophobic interactions between neutral sulfanilamide and hydrophobic silica surfaces, as already found in previous works (Fukahori et al., 2013).

Such acid-base reaction occurs with slight different modalities over the surface of the three different magnetic adsorbents. As far as SMA_LacBen magnetic adsorbent is concerned, the acid-base reaction occurs between the acidic silanol groups (Si-O-H) of the adsorbent and the basic amine group of sulfanilamide. This reaction attains its maximum at pH = 4.0. At this pH the following two opposite trends exactly balance each other:

1) at pH < 4.0 the basic amine group of sulfanilamide turns out protonated to a too large extent and, thus, creates hydrogen bonds with the silanol groups of the magnetic adsorbent SMA_LacBen to a lower extent, which results in lower sulfanilamide adsorption;
2) at pH > 4.0 the concentration of hydroxonium ion is lower and, thus, is sufficient to bridge the silanol groups of SMA_LacBen with the basic amine group of sulfanilamide to a lower extent, which also results in lower sulfanilamide adsorption.

Adsorption of sulfanilamide on (Fe,H)A800C–0min, (Fe,H)A600C–90min magnetic adsorbents occurs through a similar mechanism. It must be evidenced that SMA_LacBen exhibits the highest SA adsorption ($9.8 \cdot 10^4$ μmol/kg) owing to the fact that this is the most acidic adsorbent. Actually, it was obtained starting from a natural rock bearing clinoptilolite of Si/Al ratio of 4.14 (Manzoli et al., 2021), whereas (Fe,H)A800C–0min, (Fe,H)A600C–90min magnetic adsorbents were obtained from zeolite A which has Si/Al = 1.00 (Baerlocher et al., 2001). Thus, the concentration of silanol groups over their surface turns out lower than the one of SMA_LacBen, which explains their lower sulfanilamide adsorption. The different of acidity between the various adsorbents explain both the lower uptake by (Fe,H)A800C–0min, (Fe,H)A600C–90min than SMA_LacBen and the fact that the maximum adsorption occurs at different pH values.

The maximum amount of adsorbed sulfanilamide increases according to the following order: (Fe,H)A600C–90min (6.00 x·10^4 µmol/kg), (Fe,H)A800C–0min (7.00 x·10^4 µmol/kg), and SMA_LacBen (9.80 x·10^4 µmol/kg). Consequently, the subsequent experiments were performed using the two magnetic adsorbents which exhibit the best results (Fe,H)A800C–0min and SMA_LacBen) at the pH of maximum adsorption (6.0 and 4.0, respectively).

3.3. Kinetic and equilibrium features of the adsorption process

The Figure 3a reports the sulfanilamide uptake by (Fe,H)A800C–0min and SMA_LacBen magnetic adsorbents (S/L ratio = 1/10,000, pH 6.0 and 4.0, respectively) from an aqueous solution exhibiting an initial sulfanilamide concentration of 40.0 µmol/L, as a function of time. Both curves show that the uptake is initially quite rapid, then gradually slows down and attains a steady state after about 4 h.

The Figure 3b reports sulfanilamide uptake from water by SMA_LacBen magnetic adsorbent (S/L ratio = 1/10,000, pH 4.0) from sulfanilamide solutions of initial concentration of 40.0 and 126 µmol/L, as a function of time. Clearly, higher steady state values of sulfanilamide uptake are attained as higher initial concentrations of sulfanilamide solution are adopted. The contact time of 4 h is sufficient to attain a steady state also for the solution of initial sulfanilamide concentration of 126 µmol/L. Consequently, the values of sulphonamide uptake or residual concentration in solution recorded under such circumstances were considered as equilibrium values in further elaborations.

The best model describing the adsorption kinetics reported in Fig. is the pseudo second-order model, which can be expressed in a linear form according to Eq. (1) (Ozacar and Sengil, 2006):

$$\frac{t}{q} = \frac{1}{k_2 * q_e^2} - \frac{t}{q_e}$$

where q_e and q are the amount of sulfanilamide adsorbed (µmol/kg) at equilibrium and at time t, respectively, k_2 is the rate constant of adsorption (kg/µmol min) and t is the time (min). The values of parameters calculated for two different concentrations of SA by using SMA_LacBen are as follows. For 40 µmol/L of SA: q_e=1.05·10^5 µmol/kg, k_2 = 0.018 (kg/µmol min), r_2 = 0.99; for 126 µmol/L of SA: q_e = 1.73·10^5 µmol/kg, k_2 = 0.057 (kg/µmol min), r_2 = 0.99. As regard (Fe,H)A800C-0min the following kinetic parameters were evaluated for 40 µmol/L concentration of SA: q_e = 7.77·10^4 µmol/kg, k_2 = 0.041 (kg/µmol min), r_2 = 0.99.

The equilibrium data, reported in the Figure 4, were satisfactorily described by the Langmuir and isotherm model, while the the results (not reported) obtained with Freundlich model were unsatisfactory, so indicating the monolayer adsorption of sulfanilamide on the magnetic nanocomposites resulting from an uniform surface energy.

The Langmuir isotherm was applied for adsorption equilibrium as shown below:

$$\frac{C_e}{q_e} = \frac{1}{Q_0 b} + \frac{C_e}{Q_0}$$

where C_e is the equilibrium concentration (μmol/L), and q_e is the amount of SA adsorbed per kilogram at equilibrium (μmol/kg). Q_0 and b are Langmuir constants related to the adsorption capacity (μmol/kg) and energy of adsorption (L/μmol), respectively. The linear plot of C_e/q_e versus C_e showed that the adsorption obeyed a Langmuir isotherm model.

Q_0 and b were determined from the slope and intercept of the plots to be $4.97 \cdot 10^5$ (μmol/kg) and $5.62 \cdot 10^{-3}$ (L/μmol), for (Fe,H)A800C–0 min, and $1.02 \cdot 10^6$ (μmol/kg) and $2.41 \cdot 10^{-3}$ (L/μmol), for SMA_LacBen, respectively. The results obtained in our investigation are very promising if compared with other studies. Wan et al. (2020) reported the ability of magnetic-activated carbon composites for sulfanilamide removal demonstrating a maximum adsorption capacity and kinetic parameters lower than those estimated by us.

3.4. Thermal analysis

The sulfanilamide was also characterized as regards DTA analysis (Figure 5a) and TG analysis (Figure 5b). The DTA curve exhibits an exothermic effect denoted by a sharp peak at about 180 °C and an endothermic effect, which occurs in the temperature range 280-340 °C and attains its maximum at about 320 °C. The TG curve exhibits a small weight loss of about 5 % in the temperature range room temperature-280 °C and then an evident weight loss of about 50 % in the temperature range 280-340 °C. For temperatures higher than this last value the weight of sulfanilamide almost linearly decrease (with a small slope) thus attaining a final weight of about 18 % of the initial value at about 1000°C.

The DTA and TG curve of sulfanilamide may be interpreted by considering that the exothermic peak at about 180 °C is due to a molecular rearrangement reaction. Such molecular rearrangement reaction results in a final product of lower enthalpy and, thus, in the release of the energy amount related to the same exothermic peak. The small weight loss in this temperature range may be reasonably ascribed to sulfanilamide evaporation.

The endothermic effect, occurring in the temperature range 280-340 °C and attaining its maximum at about 320 °C, is related to the thermal decomposition of sulphonamide molecule. This interpretation is confirmed by the TG curve, which records a mass reduction of more than 50 % in this temperature range.

The features of the DTA and TG curve suggested a simple thermal regeneration method of the exhausted magnetic adsorbents. Actually, the magnetic adsorbents bearing adsorbed sulfanilamide was incubated at 400 °C for 10 min under inert nitrogen atmosphere. Such a thermal treatment, though not producing any structural variation in the magnetic adsorbent, yielded a full removal of the antibiotic. In facts, once the thermal treatment was completed, the sulfanilamide uptake by the regenerated magnetic adsorbent was about 99% of the uptake obtained using the fresh material.

4. Conclusions

Three tailor-made magnetic metal-ceramic nanocomposites, obtained from zeolite A and from a natural clinoptilolite, have been developed by thermal treatments of heavy-metal cation-exchanged zeolites at relatively moderate temperatures under a reducing atmosphere. The nanocomposites have been successfully tested to remove sulfanilamide (SA), a sulfonamide antibiotic of common use, from water.

The adsorption behaviours of the nanocomposites has been characterized, showing that the efficìency of the magnetic adsorbents strongly depends on pH. This indicates that the adsorption mechanism is affected by acid-base reactions, being sulfanilamide subjected to two acid-base processes, due to the protonation and the deprotonation of the amino and sulfonamide groups.

The exhausted adsorbent has been subject to a regeneration procedure, developed on the basis of DT and TGA analyses, allowing the complete removal of the sulfanilamide and the proper recycle of the magnetic adsorbents.

The results obtained are encouraging, demonstrating that sorption by magnetic metal-ceramic nanocomposites obtained from zeolites is a technically and economically feasible method for sulfa drugs removal.

Declaration of Competing Interest

The authors report no declarations of interest.

References

Addorisio V., Pirozzi D., Esposito S., Sannino F., 2011. Decontamination of waters polluted with simazine by sorption on mesoporous metal oxides. Journal of Hazardous Materials 196, 242-247. https://doi.org/10.1016/j.jhazmat.2011.09.022

Albino V., Cioffi R., Pansini M., Colella C., 1995. Disposal of lead-containing zeolite sludges in cement matrix. Environ. Technol. 16, 147-156. https://doi.org/10.1080/09593331608616255.

Baerlocher C., Meier W.M., Olson D.H., MAZ. Atlas of the zeolite framework types, Elsevier, Amsterdam, 2001.

Barrera G., Allia P., Bonelli B., Esposito S., Freyria F.S., Pansini M., Marocco A., Confalonieri G., Arletti R., Tiberto P., 2020. Magnetic behavior of Ni nanoparticles and Ni^{2+} ions in weakly loaded zeolitic structures. J. Alloys Compd. 817, 152776-152786. https://doi.org/10.1016/j.jallcom.2019.152776 .

Barrera G., Tiberto P., Allia P., Bonelli B., Esposito S., Marocco A., Pansini M., Leterrier Y., 2019. Magnetic properties of nanocomposites. Appl. Sci. 9, 212-240. https://doi.org/10.3390/app9020212 .

Barrera G., Tiberto P., Esposito S., Marocco A., Bonelli B., Pansini M., Manzoli M., Allia P., 2018. Magnetic clustering of Ni^{2+} ions metal-ceramic nanocomposites obtained from Ni-exchanged zeolite precursors. Ceram. Int. 44, 17240-17250. https://doi.org/10.1016/j.ceramint.2018.06.182 .

Basile A., Cacciola G., Colella C., Mercadante L., Pansini M., 1992. Thermal conductivity of natural zeolite-PTFE composites. Heat Recover. Syst. CHP 12, 497-503. https://doi.org/10.1016/0890-4332(92)90018-D .

Blasioli S., Martucci A., Paul G., Gigli I., Cossi, Johnoston C.T., Marchese I., Braschi I., 2014. Removal of sulfamethoxazole sulfonamide antibiotic from water by high silica zeolites: A study of the involved host-guest interactions by a combined structural, spectroscopic, and computational approach. J. Coll. Interf. Sci. 419, 148-159. https://doi.org/10.1016/j.jcis.2013.12.039 .

Boreen A.L., Arnold W.A., McNeill K., 2004. Photochemical fate of sulfa drugs in the aquatic environment: sulfa drugs containing five-membered heterocyclic groups. Environ. Sci. Technol. 38, 3933-3940. https://doi.org/10.1021/es0353053.

Braschi I., Paul G., Gatti G., Cossi M., Marchese L., 2013. Embedding monomers and dimers of sulfonamide antibiotics into high silica zeolite Y: an experimental and computational study of the tautomeric forms involved. RSC Advances 3, 7427-7437.

https://doi.org/10.1039/C3RA22290J .

Breck D.W.. Zeolite Molecular Sieves: structure, Chemistry, and Use. J. Wiley & Sons Ed., New York (USA), 1974.

Cappelletti P., Rapisardo G., De Gennaro B., Colella A., Langella A., Graziano S.F., Bish D.L., De Gennaro M., 2011. Immobilization of Cs and Sr in aluminosilicate matrices derived from natural zeolites. J. Nucl. Mater. 414, 451-457. https://doi.org/10.1016/j.jnucmat.2011.05.032 .

Cioffi C., Pansini M., Caputo D., Colella C., 1996. Evaluation of mechanical and leaching properties of cement-based solidified materials encapsulating Cd-exchanged natural zeolites. Environ. Technol. 11, 1215-1224. https://doi.org/10.1080/09593331708616491 .

Colella C., De' Gennaro M., Langella A., Pansini M., 1998. Evaluation of natural phillipsite and chabaziteas cation exchangers for copper and zinc. Sep. Sci. Technol. 33 () 467-481. https://doi.org/10.1080/01496399808544991 .

Colella C., Pansini M., 1988, Lead Removal for Wastewaters Using Chabazite Tuff. ACS Symposium Series; Publ by ACS, pp. 500-510.

Conde-Cid M., Cela-Doblanca R., Ferreira-Coelho G., Fernadez-Calvino D., Nuñez-Delgado A., Fernandez-Sanjurjo M.J., Arias-Estevez M., Alvarez-Rodriguez E., 2021. Sulfadiazine, sulfamethazine and sulfachloropyridazine removal using three different porous materials: Pine bark,"oak ash" and mussel shell. Env. Res. 195. 110814-110820. https://doi.org/10.1016/j.envres.2021.110814.

de Gennaro R., Langella A., D'Amore M., Dondi M., Colella A., Cappelletti P., de' Gennaro M., 2008. Use of zeolite-rich rocks and waste materials for the production of structural lightweight concretes. Appl. Clay Sci. 41, 61-72. https://doi.org/10.1016/j.clay.2007.09.008 .

De Gisi S., Lofrano G., Grassi M., Notarnicola M., 2016. Characteristics and adsorption capacities of low-cost sorbents for wastewater treatment: A review. SM&T 9, 10-40. https://doi.org/10.1016/j.susmat.2016.06.002 .

Dekhi-Bemani Y., Mir Leilabady N., Fu M., Rietveld L.C., van der Hoek J.P., Heyman S.G.J., 2021. Simultaneous removal of ammonium ions and sulfamethoxazole by ozone regenerated high silica zeolites. Wat. Res. 188, 116472-116481. https://doi.org/10.1016/j.watres.2020.116472

Dibner J.J., Richards J.D., 2005. Antibiotic growth promoters in agriculture: hitory and mode of action. Poult. Sci. 84, 634-643. https://doi.org/10.1093/ps/84.4.634 .

Directive 2013/39/EU of the European Parliament and of the Council of 12, Amending directives 2000/60/EC and 2008/105/EC as regards priority substances in the field of water policy. Off. J. Eur. Union L226, 2013, 1–17.

Dwyer F.G.. An Introduction to Zeolite Molecular Sieve. J. Wiley & Sons Ed., Chichester (UK), 1988.

Esposito S., Dell'Agli G., Marocco A., Bonelli B., Allia P., Tiberto P., Barrera G., Manzoli M., Arletti R., Pansini M., 2018. Magnetic metal-ceramic nanocomposites obtained from cation-exchanged zeolite by heat treatment in reducing atmosphere. Microporous Mesoporous Mater. 268, 131-143. https://doi.org/10.1016/j.micromeso.2018.04.024 .

Esposito S., Marocco A., Bonelli B., Pansini M., PCT international application published under Number WO**2015**/145230 A1.

Esposito S., Marocco A., Bonelli B., Pansini M., Produzione di Materiali Compositi Metallo-Ceramici Nano Strutturati da Precursori Zeolitici. Brevetto Italiano, MI**2014**A000522.

Esposito S., Marocco A., Dell'Agli G., Bonelli B., Mannu F., Allia P., Tiberto P., Barrera G., Pansini M., 2020. Separation of biological entities from human blood by using magnetic nanocomposites obtained from zeolite precursors. Molecules 25, 1803-1821. https://doi.org/10.3390/molecules25081803 .

Esposito S., Sannino F., Pansini M., Bonelli B., Garrone E., 2013. Modes of interaction of simazine with the surface of model amorphous silicas in water. J. Phys. Chem. C 117, 11203-11210. https://doi.org/10.1021/jp401997s.

Freyria F.S., Marocco A., Esposito S., Bonelli B., Barrera G., Tiberto P., Allia P., Oudayer P., Roggero A., Matéo-Vélez J.C., Dantras E., Pansini M., 2019. Simulated Moon agglutinates obtained from zeolite precursor by means of a low-cost and scalable synthesis method. ACS Earth Sp. Chem. 3, 1884-1895. https://doi.org/10.1021/acsearthspacechem.9b00042.

Fukahori S., Fujiwara T., Funamizu N., Matsukawa K., Ito R., 2013. Adsorptive removal of sulfonamide antibiotics in livestock urine using the high-silica zeolite HSZ-385. Water Sci Technol. 67.2, 319-325. https://doi.org/10.2166/wst.2012.513.

Kassinos D.F., Meric S., Nikolaou A., 2011. Pharmaceutical residues in environmental waters and wastwater: current state of knowledge and future research. Anal. Bioanal. Chem. 399, 251-275. https://doi.org/10.1007/s00216-010-4300-9.

Manzoli M., Tammaro O., Marocco A., Bonelli B., Barrera G., Tiberto P., Allia P., Matéo-Vélez J.C., Roggero A., Dantras E., Arletti R., Pansini M., Esposito S., 2021. New insights in the production of simulated moon agglutinates: the use of natural zeolite-bearing rocks. ACS Earth Space Chem. 5, 1631-1646. https://doi.org/10.1021/acsearthspacechem.1c00118 .

Marocco A., Dell'Agli G., Esposito S., Pansini M., 2012. Metal-ceramic composite materials from zeolite precursor. Sol. St. Sc. 14, 394-400. https://doi.org/10.1016/j.solidstatesciences.2012.01.006 .

Marocco A., Dell'Agli G., Sannino F., Esposito S., Bonelli B., Allia P., Tiberto P., Barrera G., Pansini M., 2020. Removal of agrochemicals from waters by adsorption: a critical comparison among humic-like substances, zeolites, porous oxides, and magnetic nanocomposites. Processes 8, 141-167. https://doi.org/10.3390/pr8020141.

Marocco A., Liguori B., Dell'Agli G., Pansini M., 2011. Sintering behaviour of celsian based ceramics obtained from the thermal conversion of (Ba, Sr)-exchanged zeolite A. J. Eur. Ceram. Soc. 31, 1965-1973. https://doi.org/10.1016/j.jeurceramsoc.2011.04.028 .

Neu H.C., Gootz T.D., Antimicrobial chemotherapy, in: S. Baron, (Ed.), Medical Microbiology, fourth ed., University of Texas Medical Branch at Galveston, Galveston (TX), 1996.

Ortiz I., Mosquera-Corral A., Rodicio J.L., Esplugas S., 2015. Advanced technologies for water treatment and reuse. AIChE J. 61, 3146-3158. https://doi.org/10.1002/aic.15013.

Ozacar M., Sengil I.A., 2006. A two stage batch adsorber design for methylene blue removal to minimize contact time. J. Environ. Manag. 80, 372-379. https://doi.org/10.1016/j.jenvman.2005.10.004 .

Pansini M., Colella C., 1990. Dynamic data on lead uptake from water by chabazite. Desalination 78, 287-295. https://doi.org/10.1016/0011-9164(90)80048-G .

Pansini M., De Gennaro R., Parlato L., De'Gennaro M., Langella A., Marocco A., Cappelletti P., Mercurio M., 2010. Use of sawing waste from zeolitic tuffs in the manufacture of ceramics. Adv. Mater. Sci. Eng. 2010, 1-9. https://doi.org/10.1155/2010/820541 .

Pansini M., Dell'Agli G., Marocco A., Netti P.A., Battista E., Lettera V., Vergara P., Allia P., Bonelli B., Tiberto P., Barrera G., Alberto G., Martra G., Arletti R., Esposito S., 2017. Preparation and charaterization of magnetic and porous metal-ceramic nanocomposites from a zeolite precursor and their application for DNA separation. J. Biomed. Nanotechnol. 13, 337-348. https://doi.org/10.1166/jbn.2017.2345 .

Pansini M., Sannino F., Marocco A., Allia P., Tiberto P., Barrera G., Polisi M., Battista E., Netti P.A., Esposito S., 2018. Novel process to prepare magnetic metal-ceramic nanocomposites from zeolite precursor and their use as adsorbent of agrochemicals from water. J. Environ. Chem. Eng. 6, 527-538. https://doi.org/10.1016/j.jece.2017.12.030 .

Pirozzi D., Imparato C., D'Errico G., Vitiello G., Aronne A., Sannino F., 2020. Three-year lifetime and regeneration of superoxide radicals on the surface of hybrid TiO_2 materials exposed to air. Journal of Hazardous Materials 387, 121716. https://doi.org/10.1016/j.jhazmat.2019.121716

Qin L.T., Pang X.R., Zeng H.H., Liang Y.P., Mo L.Y., Wang D.Q., Dai J.F., 2020. Ecological and human health risk of sulfonamides in surface water and groundwater of Huixian karst wetland in

Guilin, China. Sci. Total Environ. 708, 134552-134561. https://doi.org/10.1016/j.scitotenv.2019.134552.

Ronchetti S., Turcato E.A., Delmastro A., Esposito S., Ferone C., Pansini M., Onida B., D. Mazza, 2010. Study of the thermal transformations of Co- and Fe- exchanged zeolites A and X by "in situ" XRD under reducing atmosphere. Mater. Res. Bull. 45, 744-750. https://doi.org/10.1016/j.materresbull.2010.02.006 .

Sabri N.A., Schmitt H., Van der Zaan B., Gerritsen H.W., Zuidema T., Rijnaarts H.H.M., Langenhoff A.A.M., 2020. Prevalence of antibiotics and antibiotic resistance genes in a wastewater effluent-receiving river in the Netherlands. J. Environ. Chem. Eng. 8. 102245-102256. https://doi.org/10.1016/j.jece.2018.03.004 .

Sannino F., Pernice P., Minieri L., Camandona G.A., Aronne A., Pirozzi D., 2015. Oxidative Degradation of Different Chlorinated Phenoxyalkanoic Acid Herbicides by a Hybrid ZrO2 Gel-Derived Catalyst without Light Irradiation. ACS Applied Materials & Interfaces *7* (1), 256-263. https://pubs.acs.org/doi/10.1021/am506031e

Sannino F., Pirozzi D., Vitiello G., D'Errico G., Aronne A., Fanelli E., Pernice P., 2014. Oxidative degradation of phenanthrene in the absence of light irradiatiion by hybrid ZrO2-acetylacetonate gel-derived catalyst. Applied Catalysis B: Environmental 156–157, 101-107. https://doi.org/10.1016/j.apcatb.2014.03.006

Sannino F., Ruocco S., Marocco A., Esposito S., Pansini M., 2012. Cyclic process of simazine removal from waters by adsorption on zeolite HY and its regeneration by thermal treatment. J. Hazard. Mat. 229-230, 354-360. https://doi.org/10.1016/j.jhazmat.2012.06.011 .

Sannino F., Ruocco S., Marocco A., Esposito S., Pansini M., 2013a. Simazine removal from waters by adsorption on porous silicas tailored by sol–gel technique. Microporous and Mesoporous Materials 180, 178-186. https://doi.org/10.1016/j.micromeso.2013.06.026

Sannino F., Ruocco S., Marocco A., Esposito S., Pansini M., 2013b. Simazine removal from waters by adsorption on porous silicas tailored by sol–gel technique. Microporous Mesoporous. Mater., 180, 178-186. https://doi.org/10.1016/j.micromeso.2013.06.026 .

Srivastava B., Jhelum V., Basu D.D., Patanjali P.K., 2009. Adsorbents for pesticide uptake from contaminated water: A review, J. Sci. Ind. Res 68, 839-850. http://nopr.niscair.res.in/handle/123456789/6128 .

Uhlemann T., Berden G., Oomens J., 2021. Preferred protonation site of a series of sulfa drugs in the gas phase revealed by IR spectroscopy. Eur. Phys. J. D 75, 1-13. https://doi.org/10.1140/epjd/s10053-020-00027-x .

van Mil, The Complete Drug Reference, Sweetman S. (Ed.). The Pharmaceutical Press, London, 2011.

Wan J., Ding J., Tan W., Gao Y., Sun S., He C., 2020. Magnetic-activated carbon composites derived from iron sludge and biological sludge for sulfonamide antibiotic removal. Environ. Sci. Poll. Res. 27, 13436-13446. https://doi.org/10.1007/s11356-020-07940-z.

Zhou Y., Meng J., Zhang M., Chen S., He B., Zhao H., Li Q., Zhang S., Wang T., 2019. Which type of pollutants need to be controlled with priority in wastewater treatment plants: Traditional or emerging pollutants?. Environ. Int. 131, 104982-104995. https://doi.org/10.1016/j.envint.2019.104982 .

LIST OF TABLES AND FIGURES

Table 1.
Chemical Physical properties of (Fe,H)A600C-90 min, (Fe,H)A800C-0 min and SMA_LacBen
From Pansini et al. (2018) and Manzoli et al. (2021)

	Magnetite	Wustite	Fe (wt %)	Amorphous phase				S_{BET} (m^2/g)	V_p (cm^3/g)	M_s (emu/g)
(Fe,H)A600C-90 min	7.1	0.2	4.8	87.1				28	0.15	12.3
(Fe,H)A800C-0 min	5.4		0.2	86.4				19	0.13	4.2
	Clinoptil.	K-feldspar	Quartz	Cristob.	Muscov. / illite	Fe^0	Amorph. phase	S_{BET} (m^2/g)	V_p (cm^3/g)	M_s (emu/g)
SMA_LacBen	13.5	17.9	7.9	2.9	1.9	0.6	55.2	27.44	0.102	160

Captions for Figures

Scheme 1 - . p-aminobenzenesulfonamide (Sulfanilamide)

Figure 1 – SEM representative images of (Fe,H)A800C–0min (A, B, C), (Fe,H)A600C–90min (D, E ,F) and SMA_LacBen (G, H, I) magnetic adsorbents.

Figure 2 – Effect of pH on the adsorption of sulfanilamide on (Fe,H)A800C–0min, (Fe,H)A600C–90min and SMA_LacBen magnetic adsorbents. S/L ratio = 1/10000, contact time = 24 h

Figure 3 - Adsorption kinetics of sulfanilamide uptake:
(a) in the presence of (Fe,H)A800C–0min and SMA_LacBen magnetic adsorbents (S/L ratio = 1/10,000, pH 4.0 and 6.0, initial sulfanilamide concentration = 40.0 µmol/L).
(b) in the presence of SMA_LacBen magnetic adsorbent (S/L ratio = 1/10,000, pH 4.0, initial sulfanilamide concentrations of 40.0 and 126 µmol/L).

Figure 4 – Adsorption isotherms of sulfanilamide

Figure 5 - DTA curve (a) and TG curve (b) of sulfanilamide

Scheme 1.

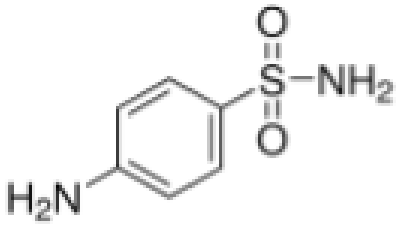

Scheme 1. *p*-aminobenzenesulfonamide (Sulfanilamide)

Figure 1.

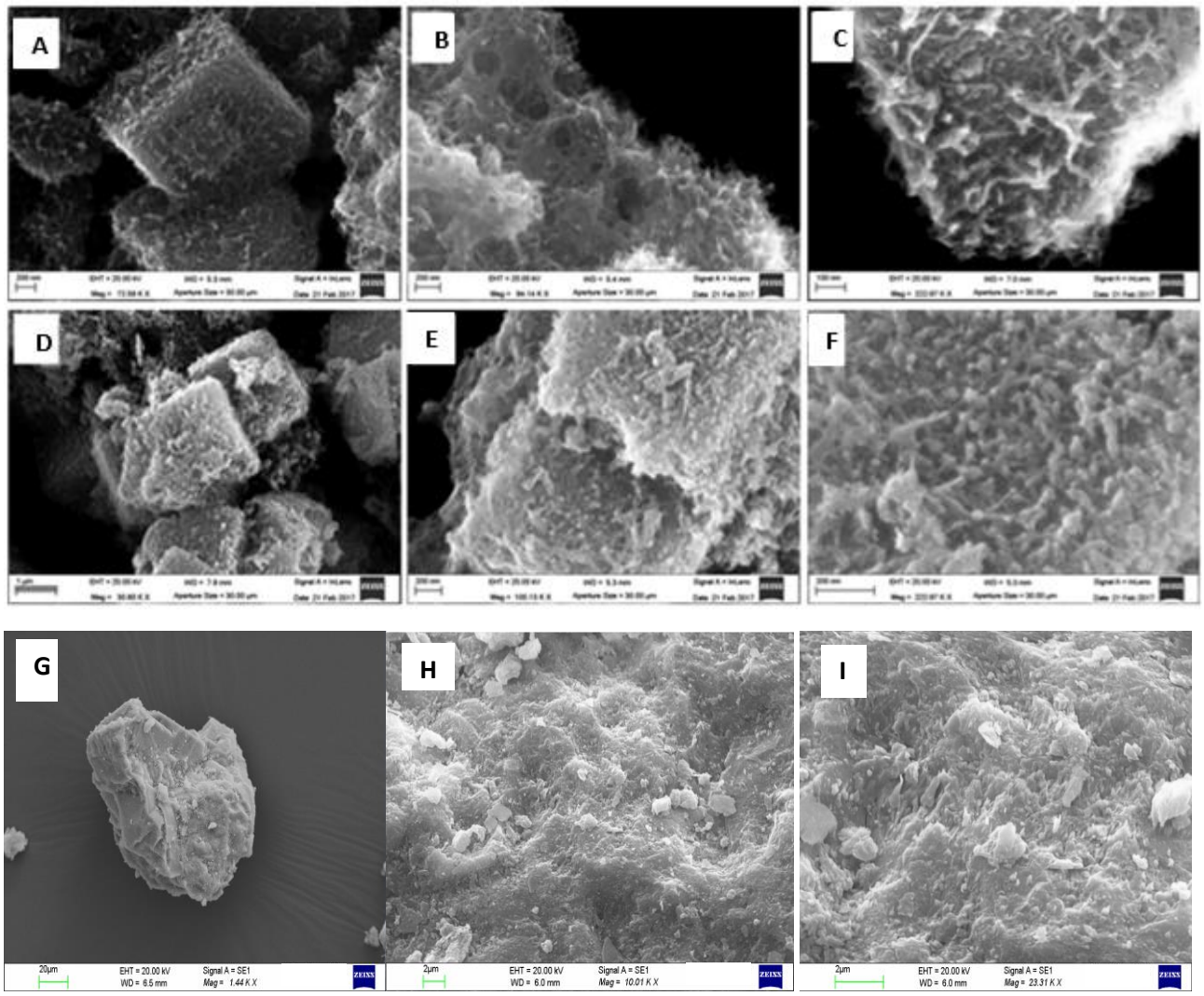

Figure 2.

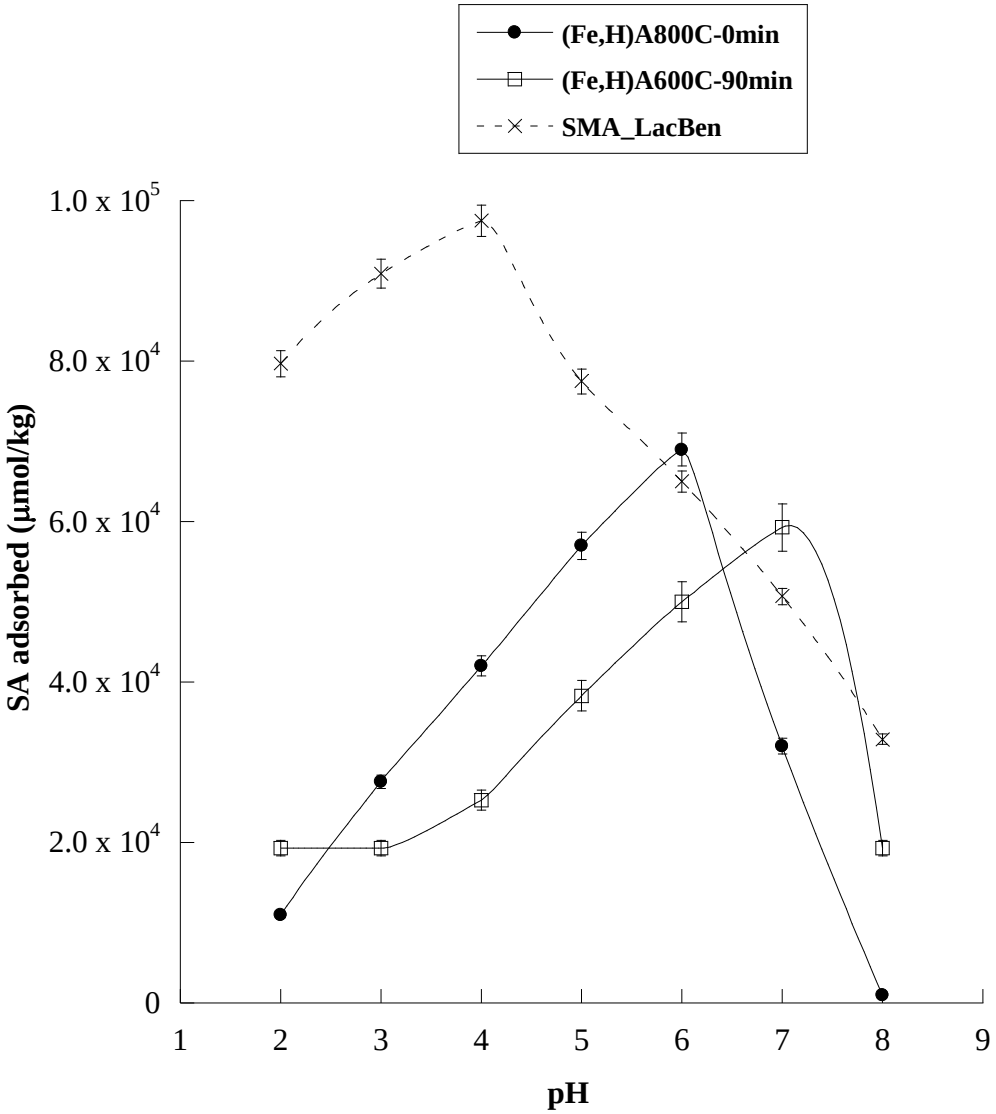
(Fe,H)A800C-0min
(Fe,H)A600C-90min
SMA_LacBen
SA adsorbed (µmol/kg)
1.0 x 10^5
8.0 x 10^4
6.0 x 10^4
4.0 x 10^4
2.0 x 10^4
0
1
2
3
4
5
6
7
8
9
pH

Figure 3a.

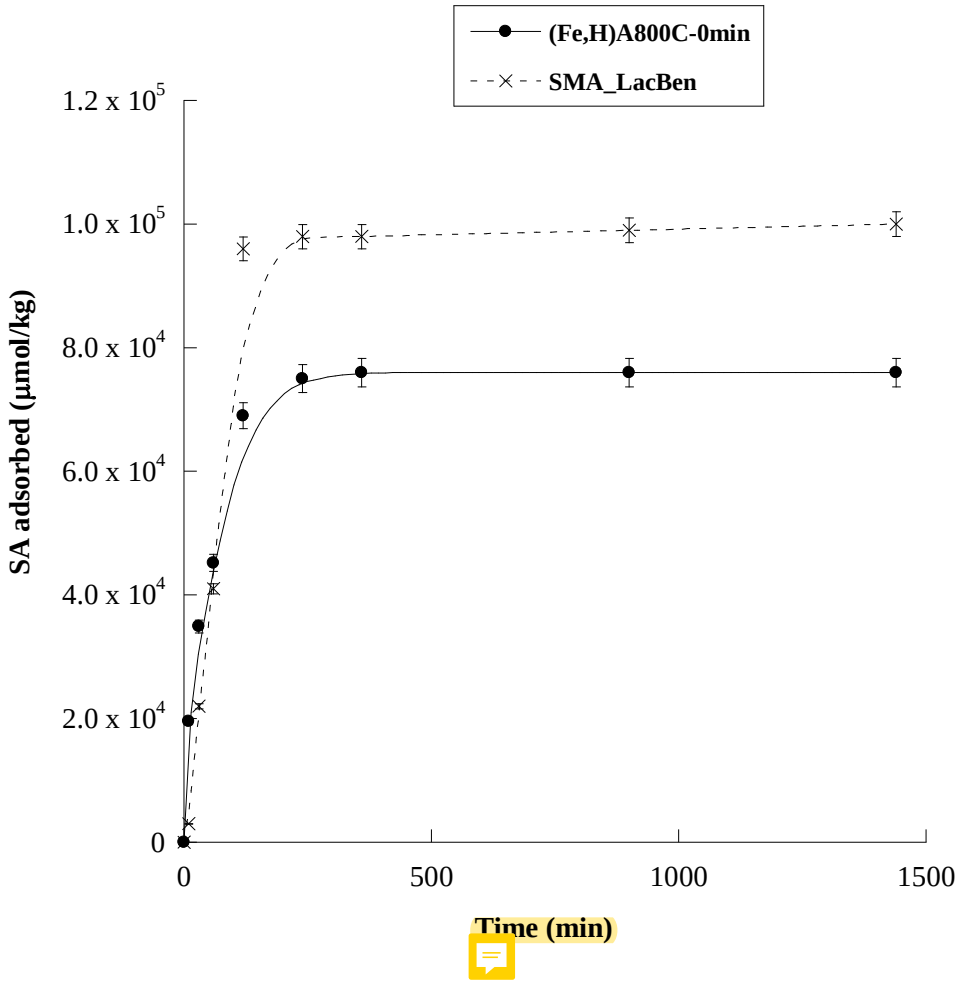
(Fe,H)A800C-0min
SMA_LacBen
SA adsorbed (µmol/kg)
1.2 x 10^5
1.0 x 10^5
8.0 x 10^4
6.0 x 10^4
4.0 x 10^4
2.0 x 10^4
0
0
500
1000
1500
Time (min)

Figure 3b.

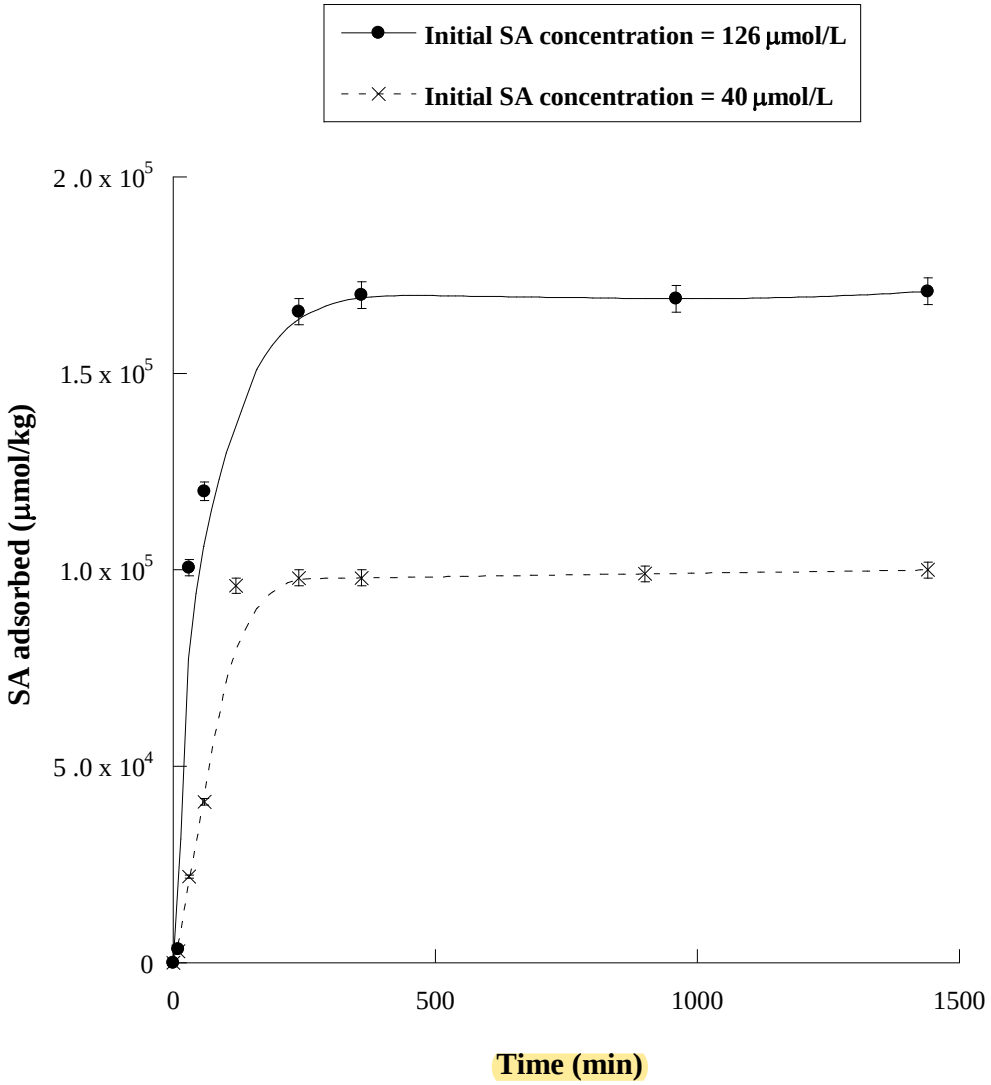
Initial SA concentration = 126 μmol/L
Initial SA concentration = 40 μmol/L
2 .0 x 10^5
1.5 x 10^5
1.0 x 10^5
5 .0 x 10^4
0
SA adsorbed (μmol/kg)
0
500
1000
1500
Time (min)

Figure 4.

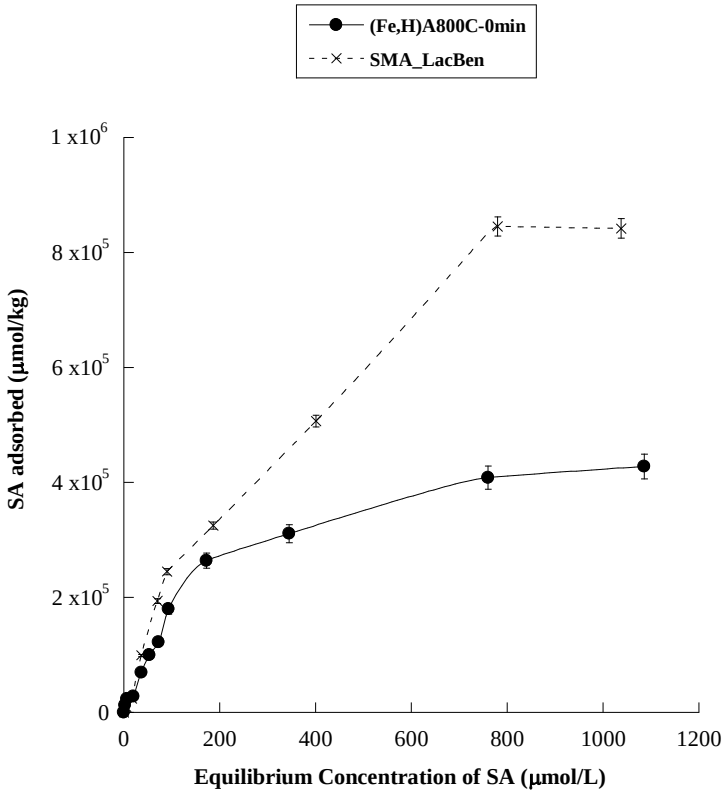
(Fe,H)A800C-0min
SMA_LacBen
1 x10^6
8 x10^5
6 x10^5
4 x10^5
2 x10^5
0
SA adsorbed (μmol/kg)
0
200
400
600
800
1000
1200
Equilibrium Concentration of SA (μmol/L)

Figure 5a.

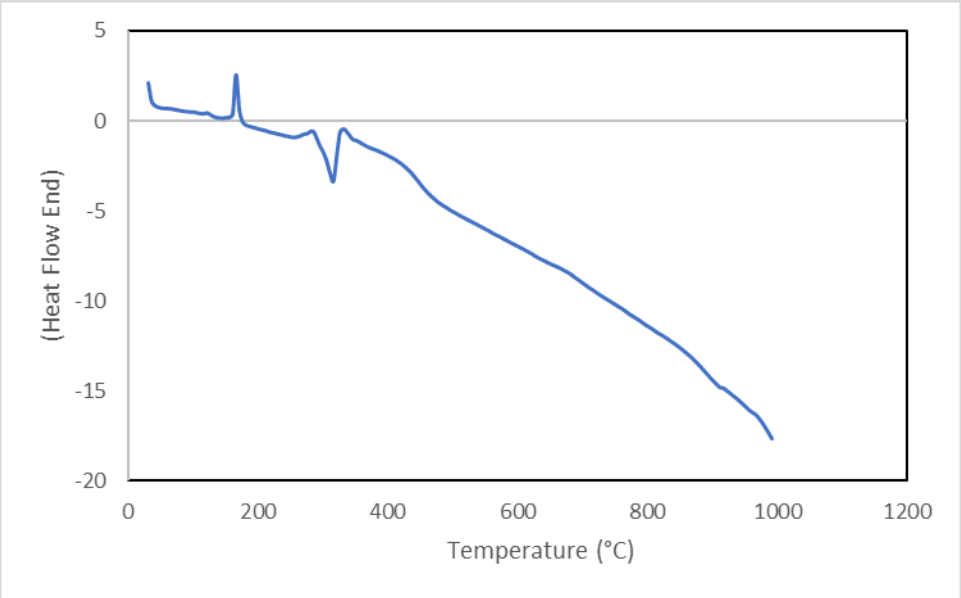

Figure 5b.